

## 1/N expansion for the degenerate Anderson model in the mixed-valence regime

F. C. Zhang and T. K. Lee

*Department of Physics, Virginia Polytechnic Institute and State University,  
Blacksburg, Virginia 24061*

(Received 14 March 1983)

The 1/N expansion method for the degenerate Anderson model is formulated.  $N$  is the degeneracy factor of one of the  $f$ -electron configurations. Various ground-state properties are calculated. Excellent agreement with the result of Bethe ansatz for  $N=6$  is shown. The rate of convergence of the series is analyzed. The merit and inadequacy of the method are discussed. At zero temperature the ratio of the magnetic susceptibility and the specific-heat linear coefficient is shown to lie within a range of 1 and  $1+(N-1)^{-1}$ .

### I. INTRODUCTION

Recently, the intermediate valence problem has aroused the interest of many physicists.<sup>1</sup> Materials containing dilute<sup>2</sup> or concentrated<sup>3</sup> rare-earth ions show similar anomalous properties. Because of the mathematical difficulty of treating the system with concentrated rare-earth ions, most theories have concentrated on understanding systems with dilute rare-earth impurities. It is generally believed that the degenerate Anderson Hamiltonian,<sup>4</sup> which modifies the original Anderson Hamiltonian<sup>5</sup> to include the orbital degeneracy of the  $f$  electrons, is a good zeroth-order model for understanding the systems with dilute mixed-valence impurities.

Exact results of the model have been obtained by using nonperturbative methods such as Bethe ansatz<sup>6-8</sup> and numerical renormalization-group methods.<sup>9</sup> Because of the difficulties of extending the above two methods to study systems with concentrated impurities, we are forced to go back to the usual diagrammatic perturbative approach. Fortunately, more than ten years ago Keiter and Kimball<sup>18</sup> prescribed the diagrammatic method for systems with dilute impurities. Recently, Grewe and Keiter<sup>11</sup> have generalized the method to treat the concentrated case.

A number of different ways to sum diagrams have been proposed.<sup>10,12,13</sup> Recently, Ramakrishnan<sup>13</sup> pointed out that due to the large value of the orbital degeneracy  $N$  of the  $f$  electrons, a more systematic and efficient way of summing diagrams is possible. This is emphasized by Anderson<sup>14</sup> as the 1/N expansion.

Several applications<sup>11,13,15</sup> of this proposed method are already published. But there is not yet a complete formulation of the 1/N expansion. A careful investigation of the merit and inadequacies of this method is required.

In this paper we present a systematic method of carrying out the 1/N expansion for the degenerate Anderson model. In Sec. II a brief introduction to the degenerate Anderson model and to the main results of the diagrammatic approach of Keiter and Kimball<sup>10</sup> are given. The formulation of the 1/N expansion for the partition function is given in Sec. III. In Sec. IV low-temperature properties such as ground-state energy, average  $f$ -electron occupation, magnetic susceptibility, and the ratio of the magnetic susceptibility and the linear specific coefficient are calculated. Excellent agreement between results of the

1/N expansion method and Bethe ansatz are achieved for the case of  $N=6$ . Dependence of the rate of convergence on the values of parameters, especially the energy level of the  $f$  electron, is analyzed. The ratio  $R$  is found to have values between 1 and  $1+(N-1)^{-1}$ . Conclusion and summary are given in Sec. V.

### II. THE DEGENERATE ANDERSON MODEL AND PERTURBATION METHODS

The degenerate Anderson model<sup>2,3</sup> for a single rare-earth impurity is given by the Hamiltonian

$$H = \sum_{k,\sigma} \epsilon_{k\sigma} C_{k\sigma}^\dagger C_{k\sigma} + \sum_m \epsilon_{fm} X_{mm} + \sum_{k,\sigma,m} V_{k\sigma m} C_{k\sigma}^\dagger X_m + \text{H.c.}, \quad (1)$$

which describes one-electron transition between a local configuration of the rare-earth impurity and the conduction-band states which are described by the annihilation operators  $C_{k\sigma}$ .  $\epsilon_{fm}$  is the energy separation between the configuration  $|m\rangle$  [with  $n-1$   $4f$  electrons in states with quantum number  $(J,m)$ ] and the configuration  $|0\rangle$  (with  $n$   $4f$  electrons in state  $J=0$ ). The projection operator  $X_m = |0\rangle\langle m|$  changes the rare-earth impurity from configurations  $|m\rangle$  to  $|0\rangle$ , and the operator  $X_{mm} = X_m^\dagger X_m = |m\rangle\langle m|$ .

For the case of  $J = \frac{1}{2}$ , this Hamiltonian is exactly the same as the conventional Anderson Hamiltonian in the limit of an infinitely large Coulomb interaction  $U$ . Crystal-field effects are neglected in this model, as they are extremely small.<sup>16</sup> Therefore, there are  $N=2J+1$  degenerate configurations  $|m\rangle$ .

A perturbative diagrammatic approach of treating the Hamiltonian has been devised by Keiter and Kimball.<sup>10</sup> Below we shall only give a very brief description of the major result of the diagrammatic method.

The hybridization interaction in Eq. (1) is treated as a perturbation, i.e.,  $H = H_0 + H'$ , and

$$H' = \sum_{k,\sigma,m} V_{k\sigma m} C_{k\sigma}^\dagger X_m + \text{H.c.} \quad (2)$$

Because the operators  $X_m$  and  $X_m^\dagger$  do not satisfy the usual anticommutation relation, one is forced to use Goldstone diagrams instead of Feynman diagrams. In general, one

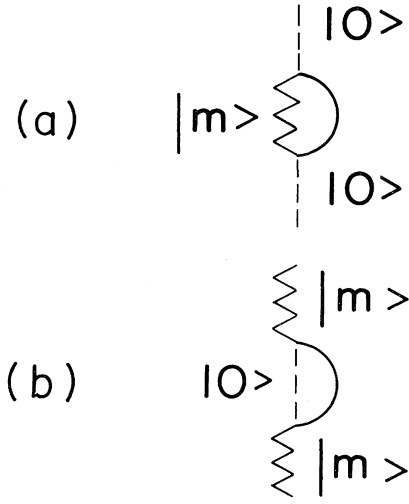


FIG. 1. Lowest-order irreducible diagrams related to energy  $E_0$  (a) and energy  $E_m$  (b).

has

$$[X_m, X_m^\dagger]_+ = X_m^\dagger X_m + \delta_{mm} X_{00}. \quad (3)$$

Detailed discussion of the operator  $X_m$  can be found in Appendix I of Ref. (10).

Keiter and Kimball<sup>10</sup> show that the series of perturbation diagrams can be summed up. The partition function can be exactly written in the following form:

$$Z = (Z_0)_c \left[ e^{-\beta E_0} + \sum_m \exp[-\beta(E_m + \epsilon_{Fm})] \right], \quad (4)$$

where  $E_0$  and  $E_m$  are the real quasiparticle energies, and  $(Z_0)_c$  is the partition function for the conduction-band states without hybridization.

The quasiparticle energies  $E_0$  and  $E_m$  are determined by self-consistent Brillouin-Wigner equations

$$E_0 = S(E_0) \quad (5)$$

and

$$E_m = T(E_m) \quad (6)$$

The self-energy functions  $S$  and  $T$  are determined from irreducible diagrams. For example, Figs. 1(a) and 1(b) lead to the following lowest-order equations:

$$E_0 = N\Delta \int d\epsilon \frac{f(\epsilon)}{E_0 - \epsilon_{Fm} + \epsilon} \quad (7)$$

and

$$E_m = \Delta \int d\epsilon \frac{1 - f(\epsilon)}{E_m + \epsilon_{Fm} - \epsilon}. \quad (8)$$

In Eqs. (7) and (8) we have defined  $\Delta$  to be

$$\Delta = \sum_{k,\sigma} |V_{k\sigma m}|^2 \delta(\omega - \epsilon_{k\sigma}).$$

In Fig. 1(a) the initial state is  $|0\rangle$  (dotted line) and the

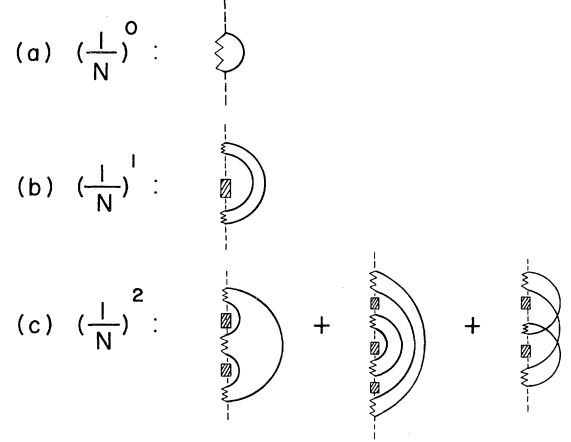


FIG. 2. Irreducible diagrams for function  $S$  [Eq. (9)] in the  $1/N$  series. The shaded block represents the lowest-order self-energy  $S_0$  [Fig. 1(a)].

intermediate state consists of  $|m\rangle$  (wavy line) and a conduction hole (straight line). Since there are  $N = 2J + 1$  degenerate intermediate states for the process of Fig. 1(a) and only one intermediate state for Fig. 1(b),  $E_0$  obtained from Eq. (7) is about  $N$  times larger than  $E_m$  of Eq. (8).<sup>13</sup>

At  $T = 0$  K, if  $-E_0 > -(E_m + \epsilon_{Fm})$ , the system has the singlet ground state with energy  $E_0$ . Therefore, a large degeneracy factor  $N$  could greatly enhance the importance of the singlet state. This leads to the suggestion by Ramakrishnan<sup>13</sup> and Anderson<sup>14</sup> that the  $1/N$  perturbative expansion may be a suitable method to treat the Hamiltonian. Indeed a rigorous  $1/N$  expansion can be carried out.

### III. $1/N$ EXPANSION

All the reducible and irreducible diagrams can be classified according to their orders in  $1/N$ . An easy way to do it is to first set the energy scale  $N\Delta = 1$ . Then the diagram of Fig. 1(a) is of order 1 and Fig. 1(b) is of order  $1/N$ . The diagrams of the same order of  $1/N$  can be summed up.

A simpler method is to work on the irreducible diagrams only. These irreducible diagrams, which constitute the self-energy functions  $S$  and  $T$  of Eqs. (5) and (6), can themselves be expanded in  $1/N$  orders. In Figs. 2 and 3 several leading-order irreducible diagrams are shown. The block represents the sum of buckle diagrams shown in Fig. 2(a); it is given by the function  $S_0$  of Eq. (15).

Once the self-energy function  $S$  is expanded in a series of  $1/N$ ,

$$S(z) = S_0(z) + N^{-1}S_1(z) + N^{-2}S_2(z) + \dots \quad (9)$$

We can also expand the energy  $E_0$  in  $1/N$  orders,

$$E_0 = E_0^{(0)} + N^{-1}E_0^{(1)} + N^{-2}E_0^{(2)} + \dots \quad (10)$$

The energies  $E_0^{(i)}$  can be determined by using the self-consistent equation (5), and we obtain

$$E_0^{(0)} = S_0(E_0^{(0)}), \quad (11)$$

$$E_0^{(1)} = S_1(E_0^{(0)})d_0, \quad (12)$$

$$E_0^{(2)} = d_0 \left[ S_2(E_0^{(0)}) + \frac{\partial S_1}{\partial E_0^{(0)}} E_0^{(1)} + \frac{\partial^2 S_0}{\partial (E_0^{(0)})^2} \frac{(E_0^{(1)})^2}{2} \right], \quad (13)$$

where

$$d_0 = \left[ 1 - \frac{\partial S_0}{\partial E_0^{(0)}} \right]^{-1}. \quad (14)$$

The functions  $S_i$  can be easily constructed, and they are given by

$$S_0(z) = \int d\epsilon f(\epsilon)(z + \epsilon - \epsilon_F)^{-1}. \quad (15)$$

$$S_1(z) = \int d\epsilon \int d\epsilon' f(\epsilon)[1 - f(\epsilon')](z + \epsilon - \epsilon_F)^{-2}[z + \epsilon - \epsilon' - S_0(z + \epsilon - \epsilon')]^{-1}, \quad (16)$$

$$S_2(z) = \int d\epsilon f(\epsilon)(z + \epsilon - \epsilon_F)^{-3} \left[ \int d\epsilon' [1 - f(\epsilon')][z + \epsilon - \epsilon' - S_0(z + \epsilon - \epsilon')]^{-1} \right]^2 + \int d\epsilon \int d\epsilon' f(\epsilon)[1 - f(\epsilon')](z + \epsilon - \epsilon_F)^{-2}[z + \epsilon - \epsilon' - S_0(z + \epsilon - \epsilon')]^{-2} S_1(z + \epsilon - \epsilon') + S_2^c(z). \quad (17)$$

The corresponding irreducible diagrams for  $S_i$  are shown in Fig. 2. The function  $S_2^c(z)$  in Eq. (17) represents the cross diagrams, the third figure in Fig. 2(c); it is given by

$$S_2^c(z) = - \int d\epsilon_1 \int d\epsilon_2 \int d\epsilon_3 f(\epsilon_1)f(\epsilon_2)f(\epsilon_3)[(z + \epsilon_1 - \epsilon_F)(z + \epsilon_3 - \epsilon_F)]^{-1} \times \{ (z + \epsilon_1 + \epsilon_2 + \epsilon_3 - \epsilon_F)[z + \epsilon_1 + \epsilon_2 - S_0(z + \epsilon_1 + \epsilon_2)][z + \epsilon_3 + \epsilon_2 - S_0(z + \epsilon_3 + \epsilon_2)] \}^{-1}. \quad (18)$$

Similarly, the self-energy function  $T$  and quasiparticle energy  $E_m$  can be expanded in a series of  $1/N$ ; they are given by

$$T(z) = N^{-1}T_1(z) + N^{-2}T_2(z) + \dots, \quad (19)$$

$$E_m(z) = N^{-1}E_m^{(1)} + N^{-2}E_m^{(2)} + \dots, \quad (20)$$

and the self-consistent equation  $E_m = T(E_m)$  becomes

$$E_m^{(1)} = T_1(0), \quad (21)$$

$$E_m^{(2)} = T_2(0) + E_m^{(1)} \left[ \frac{\partial T_1}{\partial z} \right]_{z=0}. \quad (22)$$

The functions  $T_1$  and  $T_2$  are of the form

$$T_1(z) = \int d\epsilon \frac{1 - f(\epsilon)}{z + \epsilon_{Fm} - \epsilon - S_0(z + \epsilon_{Fm} - \epsilon)}, \quad (23)$$

$$T_2(z) = \int d\epsilon \frac{[1 - f(\epsilon)]S_1(z + \epsilon_{Fm} - \epsilon)}{[z + \epsilon_{Fm} - \epsilon - S_0(z + \epsilon_{Fm} - \epsilon)]^2}.$$

The diagrams of  $T_1$  and  $T_2$  are shown in Figs. 3(a) and 3(b). Higher-order functions  $S_3, S_4$  and  $T_3, T_4$  can also be written down straightforwardly. In fact, it is easy to see that if all the cross diagrams such as  $S_2^c$  are neglected, the

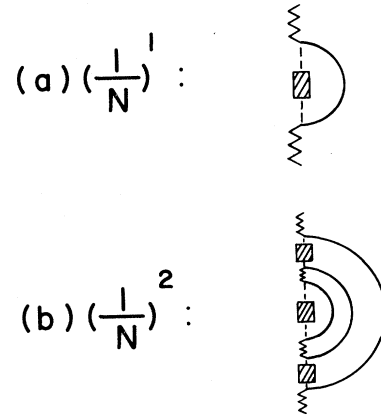


FIG. 3. Irreducible diagrams for function  $T$  [Eq. (19)] in the  $1/N$  series.

functions  $S$  and  $T$  are related through the integral equations<sup>10,17</sup>

$$S(z) = \int d\epsilon \frac{f(\epsilon)}{z + \epsilon - \epsilon_{Fm} - T(z + \epsilon - \epsilon_{Fm})}, \quad (24)$$

$$T(z) = N^{-1} \int d\epsilon \frac{1 - f(\epsilon)}{z + \epsilon_{Fm} - \epsilon - S(z + \epsilon_{Fm} - \epsilon)}.$$

By substituting Eqs. (9) and (19) into Eq. (24) and making the  $1/N$  expansion we easily obtain functions  $S_i$  and  $T_i$  (excluding the cross terms). Doing such an expansion, we realize that the  $1/N$  expansion can be valid only if  $|E_0^{(0)} - \epsilon_{Fm}| > |T|$  and the function  $T$  is of the order of  $E_m \simeq N^{-1}E_0^{(0)}$ . Therefore, qualitatively speaking, as long as  $|E_0^{(0)} - \epsilon_F| \gg N^{-1}E_0^{(0)}$ ,  $1/N$  expansion can be carried out.

In principle, if the cross terms are negligible (Appendix), the integral equations of Eq. (24) would give a more accurate result than the  $1/N$  expansion method. In practice, a very complicated regularization procedure<sup>10</sup> is required to get rid of accidentally vanishing energy denominators in Eq. (24). Czycholl<sup>17</sup> *et al.* have recently discussed such a problem. In a separate paper<sup>18</sup> planned for future publication, we will show that at zero temperature the regularization problem can be surpassed and the

ground-state energy can be calculated numerically. Because of the regularization problem, to solve Eq. (24) by iteration becomes cumbersome and difficult. On the other hand, the  $1/N$  expansion method, which is in fact a systematic way of solving the integral equation, has a simple regularization procedure. For  $N=6$  the results of the two methods are essentially identical.<sup>18</sup>

To evaluate the integrals of Eqs. (15)–(17) at zero temperature, the simple requirement of taking the principle value of the integrals is sufficient. We are restricted to the regime  $E_0^{(0)} - \epsilon_F < 0$ . To avoid unphysical divergence, the second integral of Eq. (17) must be combined with the second term of Eq. (13) and they must be evaluated together.

For the cases in which  $E_0$ , and not  $E_m + \epsilon_F$  is the ground-state energy [Eq. (4)], this  $1/N$  expansion method is a very fast converging method for calculating all the ground-state properties. Numerical results and comparison with other calculations are discussed in the following section. But for the cases in which  $\epsilon_F$  is very much below the Fermi energy, such that the ground-state energy is  $E_m + \epsilon_{Fm}$ , the advantage of having a large degeneracy factor  $N$  would be useful only for evaluating the ground-state energy, but not the magnetic susceptibility. Since in low temperatures the probability that the impurity is in the configuration  $|0\rangle$  is very small, the spin-flip-like excitation  $|m\rangle \rightarrow |m'\rangle$  would be dominant. It is well known that any finite summation of the perturbation series will always lead to divergent results for the magnetic susceptibility and other quantities, once the Kondo spin-flip interaction becomes important. Therefore, we can conclude that the  $1/N$  expansion is only partially useful to the systems which have  $E_m + \epsilon_{Fm} < E_0$ .

#### IV. NUMERICAL RESULTS

In this paper we shall only report results calculated for the ground-state properties. The numerical results for finite temperature will be presented somewhere else. Accurate results for ground-state properties would guarantee better results for finite temperature since we are doing a rigorous perturbation expansion. Under the condition  $-E_0 < E_m - \epsilon_F$  and at  $T=0$  K, Eqs. (10)–(17) have been used to calculate the following quantities: the ground-state energy  $E_0$ , the average occupation number

$$\langle n_f \rangle = \frac{\partial E_0}{\partial \epsilon_F}, \quad (25)$$

the magnetic susceptibility

$$\chi_s = - \left[ \frac{\partial^2 E_0}{\partial H^2} \right]_{H=0}, \quad (26)$$

and the coefficient of linear specific heat

$$\gamma = C_v/T = - \left[ \frac{\partial^2 E_0}{\partial T^2} \right]_{T=0}. \quad (27)$$

In the numerical calculations we have assumed constant density of states. The Fermi level is at the center of the band  $(-D, D)$ .

In Figs. 4(a) and 4(b) the ground-state energy and the average  $f$ -electron occupation  $\langle n_f \rangle$  are plotted as a function of  $\epsilon_F/D$  for the case  $N=6$  and the bandwidth

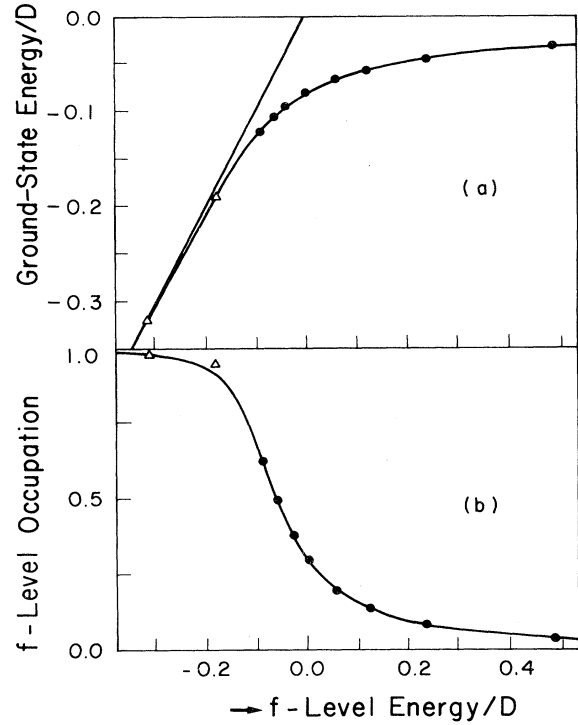


FIG. 4. Ground-state energy (a) and the average  $f$ -electron occupation (b), as a function of  $\epsilon_F/D$ :  $D=32.9N\Delta$ ,  $N=6$ . The curve is obtained from the solution of Bethe ansatz by Schlottmann (Ref. 8). The dots are for ground states with energy  $E_0/D$  [Eq. (10)], the triangles are for  $(\epsilon_F + E_m)/D$  [Eq. (20)].

$D=32.9N\Delta$ . The solid line is the result obtained from the solution of Bethe ansatz by Schlottmann.<sup>8</sup> The results of the  $1/N$  expansion are shown in dots ( $E_0$ ) and triangles ( $\epsilon_F + E_m$ ). Excellent agreement between the two results is obtained.  $E_0$  (dots) is calculated to an order of  $N^{-2}$ .  $E_m + \epsilon_F$  (triangles) is calculated to an order of  $N^{-1}$ . We have also calculated the charge susceptibility  $\chi_c = -\partial^2 E_0 / \partial \epsilon_F^2$ ; the result is again in good agreement with Schlottmann.

In order to see the rate of convergence, in Table I we list values of  $E_0^{(0)}$ ,  $N^{-1}E_0^{(1)}$ , and  $N^{-2}E_0^{(2)}$  for several values of  $\epsilon_F$ . The energy unit is  $N\Delta$ . The contribution of the cross diagram  $E_0^c$ , given by Eq. (18), is also listed. As shown in the Appendix,

$$E_0^c \approx 2N^{-2}(E_0^{(0)} - \epsilon_F - 1)^{-2}.$$

If the bandwidth is larger, the convergent rate would be faster and the contribution of the cross term would be smaller. The more negative the value  $\epsilon_F$  is, the slower the convergent rate will be. This agrees with the comment made at the end of the last section. As the value  $|E_0^{(0)} - \epsilon_F|$  becomes smaller, the expansion of the denominator of the function  $S$  in Eq. (24) becomes more and more inaccurate. Many numbers of terms need to be calculated.

In Table II the magnetic susceptibility  $\chi_s$  calculated in the  $1/N$  series is listed. The susceptibility is expressed in

TABLE I. Ground-state energy  $E_0$  in the  $1/N$  series [Eq. (11)] for  $N=6$  and  $D/N\Delta=32.9$ . The energy unit is  $N\Delta$ .  $E_0^{(0)}/N^2$  is the contribution from the cross diagram given by  $S_2^c$  of Eq. (18).

$\epsilon_F$	$E_0^{(0)}$	$E_0^{(1)}/N$	$E_0^{(2)}/N^2$	$E_0$	$E_0^{(0)}/N^2$
2.0	-2.182	-0.064	-0.002	-2.248	0.002
0.0	-2.610	-0.105	-0.004	-2.719	0.004
-1.0	-2.905	-0.139	-0.006	-3.050	0.006
-2.5	-3.512	-0.217	-0.005	-3.734	0.013

units of  $\mu^2 g^2 J(J+1)/3N\Delta$ .  $\chi_s^c$  is the contribution from the cross diagram of Eq. (18).  $\chi_s$  increases as  $\epsilon_F$  decreases; this agrees with what has been observed by Krishna-murthy *et al.*<sup>19</sup> Compared to the ground-state energy listed in Table I, the magnetic susceptibility converges a little more slowly. The first-order correction  $N^{-1}\chi_s^{(1)}$  is always quite important. The spin-flip-like interaction starts in  $N^{-1}$  order [Fig. 2(b)]. The convergent rate becomes slower when the value of  $\epsilon_F$  decreases.

We have also calculated the ground-state energy  $E_0$  and the magnetic susceptibility  $\chi_s$  for the case  $N=2$ . In general,  $E_0$  converges to a few percent after  $N^{-2}E_0^{(2)}$  is included, but  $\chi_s$  can be off by 40% for a very negative value of  $\epsilon_F$ .

The specific-heat coefficient also can be calculated straightforwardly. But we shall only discuss the ratio  $R = \chi_s/\gamma$ .  $\gamma$  is in units of  $\pi^2 k_B^2/3N\Delta$ . By using Eqs. (11), (26), and (27), both  $\chi_s$  and  $\gamma$  may be expanded in a series of  $1/N$ . Therefore, we can write  $R$  in the form

$$R = (\chi_s^{(0)} + N^{-1}\chi_s^{(1)} + \dots) / (\gamma^{(0)} + N^{-1}\gamma^{(1)} + \dots). \quad (28)$$

It is easy to show that

$$\chi_s^{(0)} = \gamma^{(0)} = (E_0^{(0)} - \epsilon_F)^{-1} (E_0^{(0)} - \epsilon_F - 1)^{-1}. \quad (29)$$

Therefore, in the limit  $N \rightarrow \infty$ ,  $R_\infty = 1$ . In the last column of Table II we have listed the values of  $R$ . They all lie within the range of 1.0 and 1.2 [ $= 1 + 1/2J = 1 + (N-1)^{-1}$ ]. For the case of  $J = \frac{1}{2}$ , Krishna-murthy *et al.*<sup>9</sup> have shown that in the mixed-valence regime,  $R$  has values between 1 and 2. In the Kondo regime,  $R = 2 = 1 + 1/2J$ . Recently, by using Bethe ansatz, Tsvelick and Wiegmann<sup>20</sup> have shown that  $R = 1 + 1/2J$  for the degenerate Kondo model. Therefore, we believe that for our model, we must have  $1 < R < 1 + 1/2J$ . Obviously, our result indeed satisfies this condition. Lustfeld and Bringer<sup>21</sup> have calculated  $R$  by using certain Brillouin-Wigner formulas. They have found that  $R < 1$ ; this is certainly incorrect. Thus we have shown that the  $1/N$  expansion method not only gives accurate results but also

has included magnetic and charge fluctuations correctly in each order, such that  $R$  is always larger than 1.

## V. CONCLUSION

We have presented a method to systematically expand the partition function or the free energy of the degenerate Anderson model in a  $1/N$  series. By using the large value of the degeneracy factor  $N$  for the  $f$  electrons, the series is shown to be quickly converging. The ground-state energy and the average  $f$ -electron occupation number  $\langle n_f \rangle$  calculated by  $1/N$  expansion are in excellent agreement with the Bethe ansatz result. The advantages and inadequacies of the method are carefully analyzed and summarized below.

For the low-temperature properties, the  $1/N$  expansion method is very efficient and accurate only if the ground-state energy is  $E_0$  and not  $E_m + \epsilon_F$ . This corresponds to the values of  $\langle n_f \rangle$  less than 0.6 or 0.7 depending on the parameters. Therefore, it is applicable for most mixed-valence compounds.

For  $N=6$ , in most cases the results of zeroth-order  $N^0$  and first-order  $N^{-1}$  expansion are accurate enough. It should be emphasized that the first-order correction, especially for magnetic susceptibility, is always quite important unless  $N$  is extremely large. Therefore, it is advisable that the first-order correction should always be taken into account.

At moderate temperatures, the method is applicable for the whole range of parameter values. We expect a better result than our low-temperature results.

Compared to other perturbative calculations<sup>12,21</sup> using certain generalized Brillouin-Wigner formulas, this method is more systematic and the error is easy to estimate. We have shown that the ratio  $R$  of the magnetic susceptibility and the linear specific-heat coefficient calculated by this method lies in the correct range, i.e., between 1 and  $1 + (N-1)^{-1}$ . Other calculations may produce incorrect values of  $R < 1$ .<sup>21</sup>

The main deficiency of this method is that it cannot

TABLE II. Magnetic susceptibility  $\chi_s$  in the  $1/N$  series. The parameters are the same as in Table I.  $\chi_s^c/N^2$  is the contribution from the cross diagram given by  $S_2^c$  of Eq. (18). The ratio  $R$  is defined in Eq. (28).

$\epsilon_F/N\Delta$	$\chi_s^{(0)}$	$\chi_s^{(1)}/N$	$\chi_s^{(2)}/N^2$	$\chi_s$	$\chi_s^c/N^2$	$R$
2.0	0.046	0.009	0.002	0.057	0.000	1.06
0.0	0.108	0.034	0.008	0.150	0.000	1.08
-1.0	0.184	0.075	0.018	0.277	-0.001	1.10
-2.5	0.498	0.355	0.050	0.903	-0.010	1.14

treat low-temperature properties in the Kondo regime of the Anderson model. This is a well-known difficulty for all the perturbative approaches. Another advantage of this method is that it can be easily generalized to treat the case of many impurities and to calculate Green functions and other dynamic quantities.

#### ACKNOWLEDGMENT

The authors wish to thank Professor S. P. Bowen for valuable assistance in the preparation of the paper.

#### APPENDIX

The contribution of the cross diagram, the third diagram of Fig. 2(c), to the ground-state energy is estimated in this Appendix. Recently Keiter<sup>22</sup> has solved the Anderson model in the zero-bandwidth limit. He has found very important contributions from the cross diagrams. Below we shall show that these contributions are negligible for a very large bandwidth.

Instead of calculating the integral  $S_2^c(z)$  of Eq. (18), we shall calculate the following integral:

$$S_2' = - \int d\epsilon_1 \int d\epsilon_2 \int d\epsilon_3 f(\epsilon_1) f(\epsilon_2) f(\epsilon_3) \\ \times [(z + \epsilon_1)(z + \epsilon_3)]^{-1} \\ \times [(z + \epsilon_1 + \epsilon_2 + \epsilon_3) \\ \times (\epsilon_1 + \epsilon_2)(\epsilon_3 + \epsilon_2)]^{-1}, \quad (\text{A1})$$

where  $z = E_0^{(0)} - \epsilon_F$  [Eqs. (14) and (18)]. At zero temperature the integration is from  $-D$  to 0. The difference between  $S_2^c$  and  $S_2'$  is the replacement of the quantity

$$E_0^{(0)} + \epsilon_2 + \epsilon_3 - S_0(E_0^{(0)} + \epsilon_2 + \epsilon_3)$$

by  $\epsilon_2 + \epsilon_3$ . Since  $S_0(E_0^{(0)}) = E_0^{(0)}$ , this replacement sets

$$S_2^c \simeq d_0^2 S_2', \quad (\text{A2})$$

where  $d_0$  is defined by Eq. (14).

By using partial fraction and partial integration, Eq. (A1) is reduced to the form

$$S_2' = \int d\epsilon_1 \int d\epsilon_2 [(z + \epsilon_1)(z + \epsilon_2)z]^{-1} \\ \times [(\epsilon_1 + \epsilon_2)^{-1} - (z + \epsilon_1 + \epsilon_2)^{-1}]. \quad (\text{A3})$$

At zero temperature regularization is not needed in evaluating Eq. (A3). The second term of Eq. (A3) is easily shown to be of the order of  $1/D$ . We shall always assume the bandwidth  $D \gg 1$  and  $D \gg z$ .

The first term of Eq. (A3) may be reduced to the following form:

$$S_2' = \int d\epsilon \{ \ln(\epsilon/D)(z + \epsilon)^{-1} z^{-2} - [\ln(\epsilon/D)]^2 z^{-2}/2 \} \\ \simeq 2z^{-2}. \quad (\text{A4})$$

By using Eqs. (14) and (15), we obtain

$$d_0 = [1 - (E_0^{(0)} - \epsilon_F)^{-1}]^{-1}. \quad (\text{A5})$$

Substitution of Eqs. (A4) and (A5) into Eq. (A2) yields

$$S_2^c \simeq 2(E_0^{(0)} - \epsilon_F - 1)^{-2}. \quad (\text{A6})$$

This result is in good agreement with the numerical result listed in the last column of Table I. Since  $E_0^{(0)}$  varies as  $\ln D$ , the cross term becomes negligible for large bandwidth.

<sup>1</sup>Valence Fluctuation in Solids, edited by L. M. Falicov, W. Hanke, and M. B. Maple (North-Holland, Amsterdam, 1981).

<sup>2</sup>W. Franz, F. Steglich, W. Zell, D. Wohlleben, and F. Pobell, Phys. Rev. Lett. **45**, 64 (1980).

<sup>3</sup>J. W. Wilkins, in Valence Fluctuation in Solids, Ref. 1., p. 459.

<sup>4</sup>B. Coqblin and J. R. Schrieffer, Phys. Rev. **185**, 847 (1969). J. H. Jefferson and K. W. H. Stevens, J. Phys. C **9**, 2151 (1976).

<sup>5</sup>P. W. Anderson, Phys. Rev. **126**, 41 (1961).

<sup>6</sup>N. Kawakami and A. Okiji, Phys. Lett. **86A**, 483 (1981); J. Phys. Soc. Jpn. **51**, 1145 (1982).

<sup>7</sup>P. B. Wiegmann, Phys. Lett. **80A**, 163 (1980); A. M. Tselick and P. B. Wiegmann, *ibid.* **89**, 368 (1982); N. Andrei, Phys. Rev. Lett. **45**, 379 (1980).

<sup>8</sup>P. Schlottmann, Z. Phys. B **49**, 109 (1982).

<sup>9</sup>H. R. Krishna-murthy, J. W. Wilkins, and K. G. Wilson, Phys. Rev. B **21**, 1044 (1980).

<sup>10</sup>H. Keiter and J. C. Kimball, Int. J. Magn. **1**, 233 (1971).

<sup>11</sup>N. Grewe and H. Keiter, Phys. Rev. B **24**, 4420 (1981).

<sup>12</sup>A. Bringer and H. Lustfeld, Z. Phys. B **28**, 213 (1977).

<sup>13</sup>T. V. Ramakrishnan, in Valence Fluctuations in Solids, Ref. 1, p. 13.

<sup>14</sup>P. W. Anderson, in Valence Fluctuations in Solids, Ref. 1, p. 451.

<sup>15</sup>O. Gunnarsson and K. Schoenhammer, Phys. Rev. Lett. **50**, 604 (1983).

<sup>16</sup>C. M. Varma, Rev. Mod. Phys. **48**, 219 (1976).

<sup>17</sup>G. Czycholl, H. Keiter, and E. Niebur, in Valence Instabilities, edited by P. Wachter and H. Boppert (North-Holland, Amsterdam, 1981).

<sup>18</sup>T. K. Lee and F. C. Zhang (unpublished).

<sup>19</sup>H. R. Krishna-murthy, K. G. Wilson, and J. W. Wilkins, Valence Instabilities and Related Narrow-Band Phenomena, edited by R. D. Parks (Plenum, New York, 1977).

<sup>20</sup>A. M. Tselick and P. B. Wiegmann, J. Phys. C **15**, 1707 (1982).

<sup>21</sup>H. Lustfeld and A. Bringer, Solid State Commun. **28**, 119 (1978).

<sup>22</sup>H. Keiter, Z. Phys. B **49**, 209 (1982).